

# Thermal nitridation of the Si(111)-(7×7) surface studied by scanning tunneling microscopy and spectroscopy

C.-L. Wu, J.-L. Hsieh, H.-D. Hsueh, and S. Gwo\*

*Department of Physics, National Tsing-Hua University, Hsinchu 300, Taiwan, Republic of China*

(Received 7 May 2001; published 2 January 2002)

By using scanning tunneling microscopy and spectroscopy (STM and STS), the initial stages of NH<sub>3</sub> exposure on Si(111)-(7×7) at different substrate temperatures and dosages have been studied. At room and very high (~1050 °C) temperatures, the 7×7 surface structure remains and the nitrated sites appear darker, randomly distributing on the surface. Moreover, we find a constant ratio (~3.46–3.83) of reacted center adatoms to reacted corner adatoms on the partially nitrated surfaces. At intermediately temperatures (~900 °C), the majority (>90%) of the reacted surface forms the well-ordered silicon nitride 8×8 reconstruction. In this regime, hexagonal- and triangular-shaped nitride islands can be observed on the 8×8 and 7×7 surfaces, respectively. We have also used STS to investigate the changes of local density of states on the nitrogen-reacted 7×7 surfaces prepared by different conditions.

DOI: 10.1103/PhysRevB.65.045309

PACS number(s): 68.37.Ef; 68.35.Bs; 77.55.+f; 81.05.Cy

## I. INTRODUCTION

Silicon nitride (Si<sub>3</sub>N<sub>4</sub>) thin films grown on the silicon surface have attracted considerable interest not only in semiconductor technology, but also in fundamental studies of surface science. Due to a nearly perfect lattice match [the 2×2 cell of the Si(111) surface is only ~1.1% bigger than the unit cell of β-Si<sub>3</sub>N<sub>4</sub>(0001)], a coherent Si<sub>3</sub>N<sub>4</sub>(0001)/Si(111) interface can be formed using the thermal nitridation process, where the Si substrate is exposed to various nitrogen-containing gases, such as NH<sub>3</sub>,<sup>1,2</sup> NO,<sup>3</sup> and N<sub>2</sub>,<sup>4</sup> or to N (Ref. 5) and ion beams<sup>6</sup> at high substrate temperatures. For thin-film applications, it is very important to know both the growth mechanism and morphology of the crystalline Si<sub>3</sub>N<sub>4</sub> films grown on the silicon surface. Previous low-energy electron diffraction (LEED) studies have reported that the Si(111)-(7×7) surface exposed to a nitrogen-containing gas exhibits either the “quadruplet” LEED pattern at high substrate temperature (above 1325 K) or the 8×8 (8×a<sub>Si(111)</sub>, a<sub>Si(111)</sub>≈3.84 Å) LEED pattern at moderately high temperatures (above 1100 K).<sup>7,8</sup> However, in most scanning tunneling microscopy (STM) studies of silicon nitride film grown on the Si(111)-(7×7) surface under 8×8 formation conditions, only the 8/3×8/3 (8/3×a<sub>Si(111)</sub>) surface hexagonal lattice could be observed.<sup>2,3,9,10</sup> On the other hand, STM studies of the partially nitrated surfaces prepared by exposing to low-dosage NH<sub>3</sub> at room temperature indicated that the 7×7 surface structure is maintained.

The experimental work reported here was undertaken to elucidate the growth mechanism and structural evolution of nitrated Si(111) surfaces at varied substrate temperature and gas dosages. We have found that NH<sub>3</sub>-reacted silicon surfaces at moderately high substrate temperatures (~900 °C) have two types of surface morphology: one is the silicon nitride terraces exhibiting 8×8 reconstruction (the dominant type); the other is the partially nitrated Si(111)-(7×7) surface with reacted 7×7 sites showing darker contrast in the STM images. For the surface prepared at a high substrate temperature (~1050 °C), a typical condition for forming the “qua-

druplet” structure, only a partially nitrated 7×7 surface can be found, indicating a silicon-rich (or nitrogen-deficient) nitride surface.

Another part of this paper is the scanning tunneling spectroscopy (STS) study of the partially nitrogen-reacted Si(111) surfaces. In the STM and STS study reported by Avouris and Wolkow,<sup>11</sup> STM images of Si(111)-(7×7) upon low dosage (~1 L) NH<sub>3</sub> at room temperature show a preferential reactivity (~3.5:1) for NH<sub>3</sub> on the center adatoms than the corner adatoms. And the STS spectra show different characteristics between the reacted sites and the unreacted sites. In our study of partially nitrated surfaces, nearly identical characteristics of STM images such as the number of reacted sites and the reactivity ratio of different adatom sites on the 7×7 surface were obtained in spite of very different NH<sub>3</sub> exposure conditions. However, the STS spectra over the partially nitrogen reacted surface show that the surface local density of states (LDOS) has extremely different features between high-temperature (~900 °C) and room-temperature exposures. It is suggested that the nitrogen atoms react with deeper silicon layers at higher temperatures.

## II. EXPERIMENT

The experiments were performed in an ultrahigh-vacuum (base pressure <1×10<sup>-10</sup> Torr) system equipped with a scanning tunneling microscope (Omicron) and a sample preparation chamber, which were separated by a gate valve. The samples were cut from a boron-doped *p*-silicon (111) wafer (ρ=0.005–0.013 Ω cm) and placed in a direct current heating molybdenum holder. Before the thermal nitridation process, the Si(111)-(7×7) reconstruction surface was obtained by repeated flashing at 1250 °C to remove native silicon oxide and other contaminants, and was then quenched to room temperature. The samples studied here did not receive any post nitridation annealing. We backfilled the NH<sub>3</sub> gas through a precision leak valve to nitrate the sample in the preparation chamber and a hot filament (temperature ≈1000 °C) placed between the leak valve and the sample surface cracked the NH<sub>3</sub> molecules to enhance reactivity.

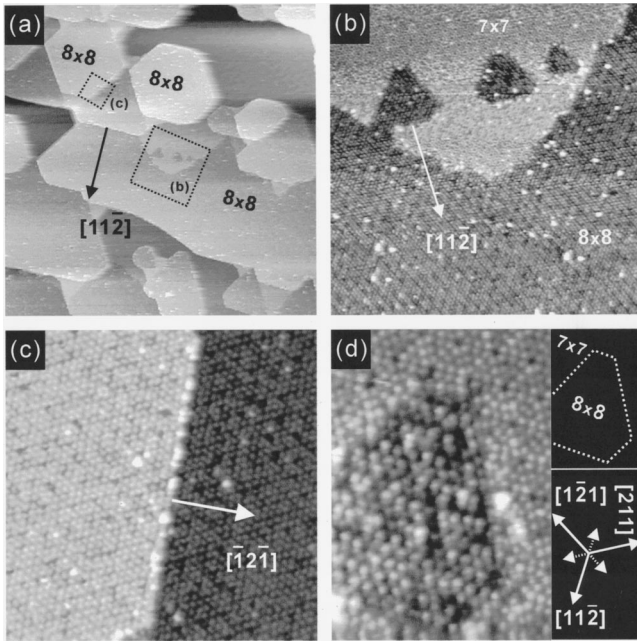


FIG. 1. Four filled-state STM images ( $V_s = -4$  V,  $I_t = 0.6$  nA) of the Si(111)-(7 $\times$ 7) surface after 12 L exposure of  $\text{NH}_3$  at the substrate temperature of 900  $^\circ\text{C}$ . (a) Large-scanning-area image (500 nm $\times$ 500 nm). Two dash-line squares are used to indicate the scanning areas of (b) and (c). (b) Upper part of the STM image (100 nm $\times$ 100 nm): three triangular-shaped 8 $\times$ 8 islands nucleated on the 7 $\times$ 7 terrace. All the edges of the triangles are along the same directions. The lower part of the image is the 8 $\times$ 8 silicon nitride reconstruction surface. (c) STM image (40 nm $\times$ 40 nm) of the 8 $\times$ 8 reconstruction terrace with a step. The step height is  $\sim 3.3$   $\text{\AA}$ , and all the 8/3 $\times$ 8/3 spots can be clearly seen. (d) Zoom-in STM image of the left triangular dark area in (b).

The nitridation temperatures were chosen to be 900 and 1050  $^\circ\text{C}$ , and the pressure—read using an ion gauge—was maintained around  $1 \times 10^{-8}$  Torr during nitridation. The actual pressure in front of the sample surface could be one order of magnitude higher than the ion gauge reading. The Langmuir number ( $L, 1 L = 1 \times 10^{-6}$  Torr s) was determined by the ion gauge reading. After the nitridation procedure, the sample was transported into the STM chamber and all STM measurements were performed at room temperature. For the STS study, normalized tunneling spectra  $[(dI/dV)/(I/V)]$  were acquired with simultaneous measurements of  $dI/dV-V$  (using a lock-in amplifier) and  $I-V$  curves while temporarily interrupting the constant-tunneling-current feedback loop.

### III. RESULTS AND DISCUSSION

#### A. (8 $\times$ 8)-reconstructed silicon nitride surface

In the initial nitridation stages, the Si(111)-(7 $\times$ 7) surface exposed to 12 L of  $\text{NH}_3$  at the substrate temperature of  $\sim 900$   $^\circ\text{C}$  transforms into two types of surface morphology as can be observed in Fig. 1 (STM filled-state images). One of them is the partially reacted surface, and the other is the silicon nitride 8 $\times$ 8 reconstruction surface (the dominant type, >90%). On the partially reacted surface, the unit cells

of the Si(111)-(7 $\times$ 7) surface still can be imaged and the reacted atomic sites appears darker in the STM images. On this type of surface, we find no evidence of nitride island nucleation. In contrast, hexagonal-or triangular-shaped completely nitrated islands are 8 $\times$ 8 reconstructed. The shapes of the silicon nitride islands are determined by the kinetics of the island growth process. The important factor, which determines the nucleation behavior, is the surface diffusion process. It is known that, for island nucleation on a sixfold symmetry lattice, the island shapes exhibit either hexagonal or triangular shape bounded by two types of steps with atomically different structures.<sup>12</sup> Figure 1(a) shows a large size (500 nm $\times$ 500 nm) filled-state STM image on a silicon nitride surface: the hexagonal silicon nitride islands with both types of steps can be clearly observed on the 8 $\times$ 8 terrace.

Figure 1(b) is an STM image (100 nm $\times$ 100 nm) taken from the central part of the large scanning-area image [Fig. 1(a)]. Both partially nitrogen reacted 7 $\times$ 7 area (upper part) and silicon nitride 8 $\times$ 8 area (lower part) can be clearly observed. It should be noted that the triangular darker areas in the 7 $\times$ 7 area have 8 $\times$ 8 reconstruction and are imaged darker due to the fact that 8 $\times$ 8 and 7 $\times$ 7 surfaces are electronically different. Therefore, the tip moved closer to the sample surface on the 8 $\times$ 8 areas in order to maintain a constant tunneling current during topography scanning. On the 7 $\times$ 7 terrace [zoom-in images shown in Figs. 1(b) and 1(d)], the island growth strongly prefers proceeding along the  $[\bar{1}1\bar{2}]$  direction and the other two threefold symmetry directions ( $[\bar{2}1\bar{1}]$  and  $[\bar{1}2\bar{1}]$ ) than the opposite  $[\bar{1}1\bar{2}]$  and corresponding threefold symmetry directions. Such a preferential nitride growth along the  $[\bar{1}1\bar{2}]$  direction on the Si(111)-7 $\times$ 7 surface was also observed previously.<sup>2,9</sup> In the STM work of Pt homoepitaxial growth by Michely *et al.*,<sup>12</sup> it was found that if the ratio of the growth speeds,  $R = \nu_{[\bar{1}1\bar{2}]} / \nu_{[\bar{1}\bar{1}2]} \cong 1$ , the shape of the nucleation island should be hexagon. On the other hand, if the geometrical shape of the nucleation islands is triangular, then  $\nu_{[\bar{1}1\bar{2}]}$  and  $\nu_{[\bar{1}\bar{1}2]}$  are not equal, i.e.,  $R \neq 1$ .

In Fig. 1(c), the unit cells of 8/3 $\times$ 8/3 spots are clearly observed and the periodicity of the spots is  $\sim 10.2$   $\text{\AA}$ . The monolayer step height of the 8 $\times$ 8 reconstruction terraces shown in Fig. 1(c) is about  $3.3 \pm 0.1$   $\text{\AA}$  [calibrated by the Si(111)-7 $\times$ 7 step height], which is significantly larger than the monolayer thickness of  $\beta$ - $\text{Si}_3\text{N}_4$  ( $\sim 2.9$   $\text{\AA}$ ) and the bilayer thickness of Si(111) ( $\sim 3.1$   $\text{\AA}$ ). The large deviation from the ideal value of  $\beta$ - $\text{Si}_3\text{N}_4$  lattice constant may result from the severe atomic relaxations to form this surface ordering. In the zoom-in STM image (Fig. 2) with a constant tunneling current of 1 nA and a sample bias of  $-4.0$  V, not only the 8/3 $\times$ 8/3 spots, but also the 8 $\times$ 8 (30.7  $\text{\AA}$  $\times$ 30.7  $\text{\AA}$ ) diamond-shaped supercells are visible with slightly detectable separations between 8 $\times$ 8 cells, and the long diagonal of the supercell aligns along the  $[\bar{1}1\bar{2}]$  direction of the Si(111) substrate. In general, the long-range ordering of the 8 $\times$ 8 periodicity is not very good. A detailed modeling for this 8 $\times$ 8 structure has been proposed recently using a combined technique of Kikuchi electron holography, high-resolution STM, and *ab initio* calculations.<sup>14</sup> In this model, the underlying structure of the nitride layer is the  $\beta$ - $\text{Si}_3\text{N}_4$  crystal and the surface 8 $\times$ 8 supercell is diamond shaped, including nine nitrogen

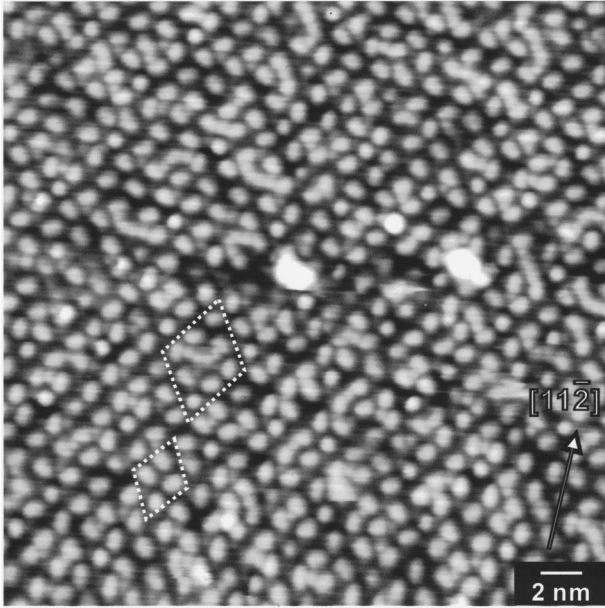


FIG. 2. 28 nm×28 nm STM image of the 8×8 silicon nitride-reconstructed surface. The sample bias was  $-4.0$  V, and the set tunneling current was 1.0 nA. Both  $8/3 \times 8/3$  and  $8 \times 8$  unit cells can be clearly observed and are indicated by two dash-line diamonds.

adatoms in each cell with an average nearest-neighbor distance of  $\sim 10 \text{ \AA}$ . Also, the  $8 \times 8$  supercell has a mirror symmetry about the  $[11\bar{2}]$  direction of the Si(111) substrate (the long diagonal of the  $8 \times 8$  diamond cell) and a mirror asymmetry about the  $[1\bar{1}0]$  direction (the short diagonal of the  $8 \times 8$  diamond cell).<sup>14</sup> In the zoom-in STM image shown in Fig. 1(d) (16 nm×23 nm), we can observe both the initial stage for forming the  $8 \times 8$  reconstruction surface and the underlying structure of the  $8 \times 8$  reconstructed surface region with missing adatoms.

### B. Partially nitrated (7×7) surfaces

After exposure of  $\text{NH}_3$  on the Si(111)-(7×7) surface, the reacted or unreacted sites of the 7×7 reconstruction surface can be easily distinguished in the STM images. Figure 3 shows the filled-state image of the surface after exposure of 50 L ammonia at room temperature, and the reacted sites are imaged with a darker contrast by STM. This image of a partially reacted surface is very similar to that reported by the Wolkow and Avouris using a low ammonia dosage at

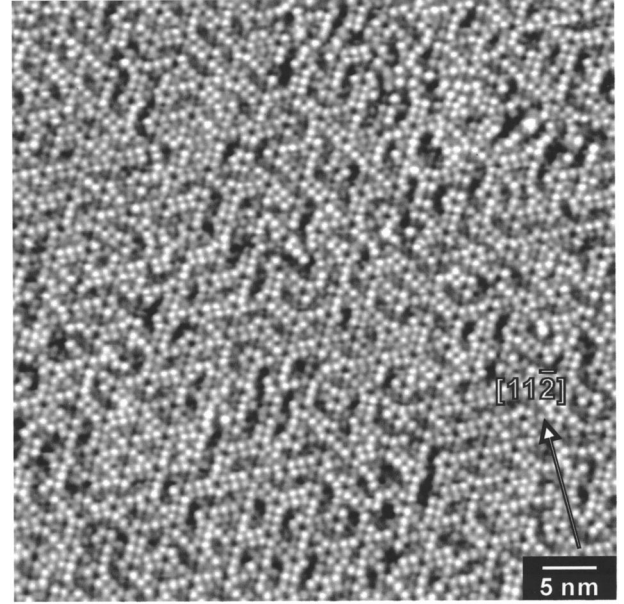


FIG. 3. A 50 nm×50 nm filled-state ( $V_s = -0.7$  V,  $I_t = 1.0$  nA) STM image of Si(111)-(7×7) surface after ammonia exposure with a low dosage (6 L) and at a high substrate temperature ( $\sim 1050$  °C).

room temperature and in agreement with their conclusion that  $\text{NH}_3$  molecules reacted preferentially on the center adatoms than on the corner adatoms of the Si(111)-(7×7) surface.<sup>1</sup> In the atom-resolved STS measurements by Wolkow and Avouris, the rest atom dangling-bond states were fully eliminated after reaction.<sup>1</sup> Since there are two rest atom neighbors for each center adatoms, while there is only one for the case of corner adatoms, it was suggested that there should be more unreacted corner adatoms than unreacted center adatoms. The topographic contrast between center and corner adatoms results from the difference in charge transfer with the neighboring rest atoms. Under the above hypothesis that  $\text{NH}_3$  molecules react only with rest atoms, the center adatom to corner adatom reactivity ratio would be 2:1. However, our experimentally observed ratio of reacted center adatoms to reacted corner adatoms, as shown in Table I, is larger than 3:1 for both room-temperature or high-temperature ammonia exposures. This is because the ammonia molecules can dissociate on the clean silicon surface even at room temperature, so a reactivity ratio larger than 2:1 should include a contribution from the H atom adsorption on

TABLE I. The ratios of reacted adatoms (dark sites) to total counted adatoms and reacted center adatoms to reacted corner adatoms.

Initial surface	Ammonia dosage	Substrate temperature	Ratio of reacted adatoms to total counted adatoms	Ratio of reacted center adatoms to reacted corner adatoms
Si(111)-(7×7)	50 L	Room temperature	0.356	3.73
Si(111)-(7×7)	12 L	900 °C	0.412 <sup>a</sup>	3.83 <sup>a</sup>
Si(111)-(7×7)	12 L	1050 °C	0.411	3.46

<sup>a</sup>Counted on the remaining 7×7 partially nitrated areas of the mainly 8×8 nitride surface.

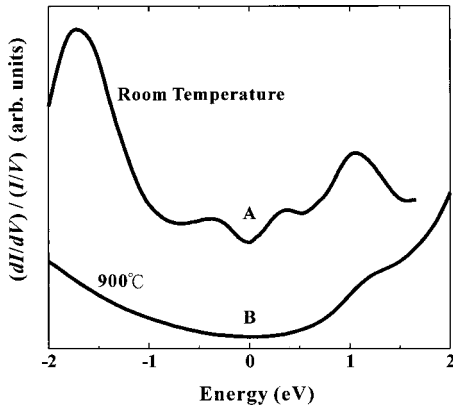


FIG. 4. The STS spectra obtained at the  $\text{NH}_3$ -exposure Si(111)-(7 $\times$ 7) surface. Curve *A* is a spectrum over the partially  $\text{NH}_3$ -reacted surface after exposure at room temperature; curve *B* is a spectrum over the partially  $\text{NH}_3$ -reacted surface, but after exposure at high temperature (900  $^\circ\text{C}$ ).

the rest atom or adatom sites during the cooling-down process with the presence of residual ammonia.

In Table I, we also show the ratios of the unreacted area to the scanned area with 50 L exposure at room temperature and 12 L exposures at high temperatures (900 and 1050  $^\circ\text{C}$ ) are 0.644, 0.588, and 0.589, respectively. Although we applied a lower exposure dosage at high temperatures than at room temperature, a larger nitrogen-reacted area ratio could be obtained at high temperatures, indicating that  $\text{NH}_3$  is more reactive with silicon at higher substrate temperatures. Also, based on the fact that the ratios of unreacted adatoms to the total adatom surface sites at 900 and 1050  $^\circ\text{C}$  in Table I are so closed ( $\sim 0.59$ ), we conclude that the reacted area would not increase further when elevating the exposure temperature above 900  $^\circ\text{C}$ . From these observations, we believe that the so-called “quadruplet” structure of high-temperature nitridation should be a silicon-rich surface with an underlying silicon nitride layer.

### C. STS results of partially and completely nitrided Si(111) surfaces

In scanning tunneling spectroscopy studies, the LDOS information can be obtained based on the fact that the quantity  $(dI/dV)/(I/V)$  is approximately proportional to the LDOS.<sup>15</sup> Using a lock-in amplifier, detection and measurement of the differential conductivity  $dI/dV$  is achieved by adding a very small ac modulation signal to the sample bias voltage. Dividing the differential conductivity  $dI/dV$  by simultaneously measured  $I/V$ , the normalized conductivity can be obtained and the dependence of  $dI/dV$  on the tip-sample separation is removed.<sup>15</sup> As a consequence, we could obtain the electronic properties of the partially nitrided silicon (7 $\times$ 7) surfaces and the 8 $\times$ 8 reconstructed silicon nitride surface from the STS spectra.

It should be noted that the STS spectra of the partially reacted surface at different temperatures are very different. Curve *A* in Fig. 4 is the STS spectrum of the room-temperature ammonia exposed surface: the peaks at  $\sim -0.3$

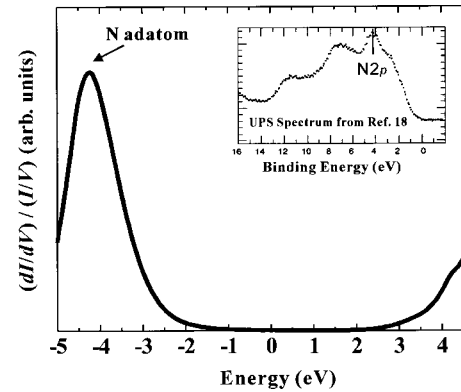


FIG. 5. The STS spectra obtained on the (8 $\times$ 8)-reconstructed silicon nitride surface. The conduction band maximum ( $E_C$ ) and the valence band minimum ( $E_V$ ) are indicated. The inset shows the UPS spectrum of  $\text{NH}_3$  reacted on a clean Si(111)-(7 $\times$ 7) surface at 1193 K (120 L) adapted from Ref. 18.

eV and  $\sim +0.25$  eV of spectrum *A* correspond to the LDOS of the adatoms,<sup>1</sup> and the peak at  $\sim -1.8$  eV is related to the back-bond state. Spectrum *B* is obtained on the high-temperature ammonia exposed surface, and all the STS spectra measured over the 15 nm $\times$ 15 nm partially reacted surface were very similar. By comparing with an ultraviolet photoemission spectroscopy (UPS) study on a Si(111)-(7 $\times$ 7) surface nitridated at 1193 K (120 L of ammonia),<sup>13</sup> there are no LDOS peaks from 0 to  $-2$  eV in either UPS spectra or our STS spectrum (curve *B* in Fig. 4). Comparing between curve *A* and curve *B* in Fig. 4, we can clearly observe that almost all the LDOS peaks of the spectrum *B* (except an unidentified state at  $\sim +1.2$  eV) are eliminated and there is a small energy band gap. We suggest the reason for the large distinction between spectrum *A* and spectrum *B* in Fig. 4 may be due to the nitrogen atoms reacting with the lower-lying silicon layers to form silicon nitride at high temperatures, so that the LDOS measurements on the silicon surface are affected by the layer of insulating silicon nitride, although the STM images are very similar for ammonia exposures at room or high temperatures. Furthermore, according to the measured band gap of spectrum *B* in Fig. 4 and the unoccupied STM 7 $\times$ 7 images, the partially reacted surfaces obtained at high substrate temperatures should be silicon-rich surfaces. In addition, it should be noted that the nitrogen atoms can react with lower silicon layers so that a quantitative interpretation of the reactivity ratio of the corner adatoms and the center adatoms at high temperature could not only consider the surface bonding, but also include the influence upon subsurface-layer nitridation of silicon.

In Fig. 5 we show the STS spectrum of the 8 $\times$ 8 silicon nitride surface, where a strong occupied LDOS at  $\sim -4.2$  eV below the Fermi level can be observed. The characteristic feature of a strong LDOS peak at  $-4.2$  eV is in agreement with the reported UPS spectra of 5 L ammonia-exposed Si(100) at 1100 K (Ref. 16) and the  $\text{NH}_3$ -chemisorbed Si(111) surface after annealing at 1000 K.<sup>17</sup> In addition,  $\text{NH}_3$  dosed (120 L) above 1000 K on Si(100)-(2 $\times$ 1) and Si(111)-(7 $\times$ 7) surfaces, the valence band spectra also exhibit the

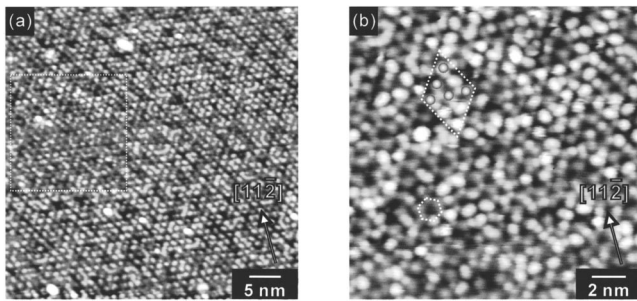


FIG. 6. STM images taken at a sample bias of  $-4.0$  V and the set tunneling current of  $1$  nA. (a) Scanning size is  $45$  nm $\times$  $45$  nm. The dash-line square region in the image is the STS measurement area, and part of nitrogen adatoms were desorbed in this region. (b)  $17$  nm $\times$  $17$  nm STM image of the square area in (a). The honeycomblike atomic “rings” (indicated by the dashed hexagonal area) can be observed in this image, and the brighter dots are the remaining nitrogen adatoms (the desorbed nitrogen adatoms are represented by gray balls in the indicated  $8\times 8$  unit cell).

$4.2$  eV peak (Ref. 18, the inset of Fig. 5). The calculations by Ren and Ching for crystalline  $\beta$ - $\text{Si}_3\text{N}_4$  indicate that the  $4.2$  eV LDOS peak is due to the nonbonding N  $2p_\pi$  orbital.<sup>19</sup> Based on the results of STS, UPS, and calculations, the imaged adatom sites on the  $8\times 8$  silicon nitride surface should be the nonbonding nitrogen orbitals.

In the STS spectra, the band gap of the  $8\times 8$  silicon nitride surface can be measured. From electronic structure calculations for crystalline  $\beta$ - $\text{Si}_3\text{N}_4$ , the indirect and direct band gap is  $4.96$  and  $5.25$  eV, respectively.<sup>20</sup> In our STS measurements, the band gap of the  $8\times 8$  silicon nitride surface is about  $4$  eV, which correspond to a wide-band-gap semiconductor surface. This is the reason why we believe that the ( $8\times 8$ )-reconstructed surface should not be modeled by the crystalline  $\beta$ - $\text{Si}_3\text{N}_4$  structure.

In addition, we observed an interesting phenomenon of electron-beam-stimulated desorption of the nitrogen adatoms on the  $8\times 8$  reconstruction surface during STS measurements. After taking the multiple STS spectra on the  $20$  nm $\times$  $20$  nm area indicated by a dashed square [Fig. 6(a)], some nitrogen adatoms disappeared and the lower layer of the silicon nitride ( $8\times 8$ )-reconstructed surface could be observed. Figure 6(b) is an STM image on the adatoms desorbed area: honeycomblike atomic “rings” (indicated by

dashed lines) can be observed, and the nondesorbed nitrogen adatoms are the brighter dots (the desorbed adatoms are also indicated by gray balls). This is another indication that the adatoms on the  $8\times 8$  reconstruction surface are nitrogen atoms because of their volatile nature during the STS measurements.

#### IV. SUMMARY

We have investigated the initial stages of thermal nitridation process on the Si(111)-(7 $\times$ 7) surface using STM and STS. In the STM studies, the  $\text{NH}_3$ -reacted silicon surfaces at moderately high substrate temperature ( $900^\circ\text{C}$ ) have two types of surface morphology: one is imaged with ( $8\times 8$ ) reconstructed silicon nitride terraces ( $>90\%$ ), and the other is the partially reacted Si(111)-(7 $\times$ 7) surface with reacted sites imaged darker and randomly distributed on the 7 $\times$ 7 terraces. For surfaces prepared at a high substrate temperature ( $1050^\circ\text{C}$ ), a typical condition for forming the “quadruplet” structure, only partially nitrated 7 $\times$ 7 surfaces can be found. According to the shapes of the silicon nitride islands, the preferential direction of the island step growth on the Si(111) surface at  $900^\circ\text{C}$  can be determined to be along the  $[\bar{1}1\bar{2}]$  directions, while  $[\bar{1}1\bar{2}]$  and  $[\bar{1}1\bar{2}]$  growth rates are identical on the  $8\times 8$  terrace. STS measurement results on the partially nitrogen-reacted surface show a strong dependence on the nitridation temperature. At room temperature, the peaks of the STS spectrum are dominated by Si surface states. However, at  $900^\circ\text{C}$ , these surface peaks on the partially nitrated 7 $\times$ 7 surface disappear and a small band gap appears in the spectrum. From these results, it is suggested that the N atoms react with lower silicon layers at moderate high substrate temperatures and the underlying silicon nitride layer can affect the surface state of the silicon-rich surface.

#### ACKNOWLEDGMENTS

We would like to thank H. Ahn, C. M. Wei, and Y. C. Chou for helpful discussions. This work was partially supported by the National Science Council, Taiwan (NSC-89-2112-M-007-093 and NSC-90-2112-M-007-059), and the Program for Promoting Academic Excellence of Universities (Contract No. 89-FA04-AA), the Ministry of Education, Taiwan.

\*Electronic address: gwo@phys.nthu.edu.tw

<sup>1</sup>R. Wolkow and Ph. Avouris, Phys. Rev. Lett. **60**, 1049 (1988).

<sup>2</sup>E. Bauer, Y. Wei, T. Müller, A. Pavlovskaya, and I. S. T. Tsong, Phys. Rev. B **51**, 17 891 (1995).

<sup>3</sup>B. Röttger, R. Kliese, and H. Neddermeyer, J. Vac. Sci. Technol. B **14**, 1051 (1996).

<sup>4</sup>E. Bauer, Y. Wei, T. Müller, A. Pavlovsky, and I. S. T. Tsong, Phys. Rev. B **51**, 17 891 (1995).

<sup>5</sup>D. V. Tsu, G. Lucovsky, and M. J. Mantini, Phys. Rev. B **33**, 7096 (1986).

<sup>6</sup>D. Bolmont, J. L. Bischoff, F. Lutz, and L. Kubler, Appl. Phys. Lett. **59**, 2742 (1991).

<sup>7</sup>A. G. Schrott and J. S. C. Fain, Surf. Sci. **111**, 39 (1981).

<sup>8</sup>A. G. Schrott and J. S. C. Fain, Surf. Sci. **123**, 204 (1981).

<sup>9</sup>J. S. Ha, K.-H. Park, W. S. Yun, Y.-J. Ko, and S. K. Kim, Surf. Sci. **426**, 373 (1999).

<sup>10</sup>Y. Morita and H. Tokumoto, Surf. Sci. **443**, L1037 (1999).

<sup>11</sup>Ph. Avouris and R. Wolkow, Phys. Rev. B **39**, 5091 (1989).

<sup>12</sup>T. Michely, M. Hohage, M. Bott, and G. Comsa, Phys. Rev. Lett. **70**, 3943 (1993).

<sup>13</sup>G. Dufour, F. Rochet, H. Roulet, and F. Sirotti, Surf. Sci. **304**, 33 (1993).

<sup>14</sup>H. Ahn, C.-L. Wu, S. Gwo, C. M. Wei, and Y. C. Chou, Phys. Rev. Lett. **86**, 2818 (2001).

- <sup>15</sup>R. M. Feenstra, J. A. Stroscio, and A. P. Fein, Surf. Sci. **191**, L756 (1987).  
<sup>16</sup>F. Bozso and Ph. Avouris, Phys. Rev. B **38**, 3937 (1988).  
<sup>17</sup>T. Isu and K. Fujiwara, Solid State Commun. **42**, 477 (1982).  
<sup>18</sup>G. Dufour, F. Rochet, H. Roulet, and F. Sirotti, Surf. Sci. **304**, 33 (1994).  
<sup>19</sup>S.-Y. Ren and W. Y. Ching, Phys. Rev. B **23**, 5454 (1981).  
<sup>20</sup>Y.-N. Xu and W. Y. Ching, Phys. Rev. B **51**, 17 379 (1995).